Article ID: 1006-8775(2017) 02-0210-07

WIND SHEAR IDENTIFICATION WITH THE RETRIEVED WIND OF DOPPLER WEATHER RADAR

ZHOU Sheng-hui (周生辉)[1, 2], WEI Ming (魏 鸣)[3], WANG Li-jun (王黎俊)[4], ZHENG Hui (郑 辉)[1], ZHANG Bo-yue (张博越)[4], LIN Chun-ying (林春英)[4]

(1. Collaborative Innovation Center on Yellow River Civilization of Henan Province, College of Environment and Planning, Henan University, Kaifeng 475004 China; 2. Qinghai Province Key Laboratory of Disaster Prevention and Reduction, Xining 810001 China; 3. Collaborative Innovation Center on Forecast and Evaluation of Meteorological Disasters, Nanjing University of Information Science & Technology, Nanjing 210044 China; 4. Weather Modification Office of Qinghai Province, Xining 810001 China)

Abstract: Wind shear reflects that the wind field is not uniform, which is one of the primary factors which make the retrieval of the wind field difficult. Based on volume velocity process (VVP) wind field retrieval technique, the intensity of wind shear is identified in this paper. After analyzing the traditional techniques that rely on the difference of radial velocity to identify wind shear, a fixed difference among radial velocities that may cause false identification in a uniform wind field was found. Because of the non-uniformity in wind shear areas, the difference of retrieved results between surrounding analysis volumes can be used as a measurement to show how strong the wind shear is. According to the analysis of a severe convective weather process that occurred in Guangzhou, it can be found that the areas of wind shear appeared with the strength significantly larger than in other regions and the magnitude generally larger than 4.5 m/(s·km). Besides, by comparing the variation of wind shear strength during the convection, it can be found that new cells will be more likely to generate when the strength is above 3.0 m/(s·km). Therefore, the analysis of strong wind shear's movement and development is helpful to forecasting severe convections.

Key words: wind shear; wind field retrieval; Doppler weather radar; conventions

CLC number: P415.2 **Document code:** A

doi: 10.16555/j.1006-8775.2017.02.009

1 INTRODUCTION

The modern weather radar can not only provide real-time observation for the heavy rainfall weather disasters, but also obtain the evolution information of the atmospheric, such as wind shear and turbulence, at the same time [1]. The wind shear, which can be used as a helpful precursor information of occurrence and maintenance of weather processes, as well as forecasting heavy rainfall, squall lines, mesoscale cyclones and typhoons [2–4]. Several tools can be used in detecting the wind shear, such as wind profile instrument, laser Doppler radar and Doppler weather radar. However, the wind profile instrument does not work very well in rainy days, even it can detect atmospheric turbulence under clear sky conditions[5]. The laser Doppler radar, which has a high revolution in observation and already been used in airports to detect low-level wind shear and atmospheric turbulence, is also affected by signal degradation and the application is limited to rain[6]. These two devices mentioned above have a shorter detection range compared with the Doppler weather radar.

According to the observation of low-level wind shear with Doppler weather radars, Uyeda and Zrnić[7] proposed an identification algorithm based on the difference of radial velocity. By comparing the velocity of the wind in prefrontal and postfrontal positions, Hermes et. al.[8] identified gust-front locations through a threshold value of 2.0m/(s·km) with the linear regression method and projection relationship between the horizontal wind field and radial velocity, and found that the discontinuity would affect the analysis in the vertical direction. Moreover, the ground clutter is another factor which could cause misjudgment in low elevations. Eilts et. al.[9] improved the revolution in the identification of weak echo areas and found that it was helpful to identify the convergence when the radial velocity was small. For the wide range of radar network observation,

Received 2015-07-16; **Revised** 2017-05-02; **Accepted** 2017-05-15

Foundation item: Qinghai province key laboratory open fund of disaster prevention and reduction (QHKF201401); Key technology projects of China Meteorological Bureau (CMAGJ2014M21); National Natural Science Fund (41675029, 41401504, 41671425, 41565008); Key Scientific Research Projects in Colleges and Universities (17A170005); China Postdoctoral Fund (2016M602232); Foundation of Henan University (2015YBZR020)

Biography: ZHOU Sheng-hui, Ph. D., associate researcher, primarily undertaking research on atmospheric remote sensing.

Corresponding author: WEI Ming, e-mail: njueducn@126.com

the NSSL (National Severe Storms Laboratory) succeeded in tracking rotations as tornado by merging data from multiple radars and calculating the azimuth shear fields [10]. Augros et. al.[11] used the data, which were collected by all radars from the France operational network, to project onto a Cartesian grid to build a mosaic of wind shear. The wind shear was obtained by the radial velocity gradient between neighbor grids and the gust front was also forecast with other parameters.

In the analysis of wind shear identification, Wang et. al. [12] studied the low-level wind shear and convergence line with Doppler weather radar's radial velocity and analyzed the effect of window size on data preprocessing and identification. Based on the second-order extended Prony model, Bai et. al. [13] proposed a detection algorithm, which could filter weak radar echoes and discriminate meteorological echoes and clutters, to detect low-level wind shear by analyzing the spectrum of radar echo data.

The wind shear is always consisted of vertical wind shear and horizontal wind shear, many wind shear identification methods are on the basis of the radial velocity, the radial velocity difference or both of them. However, in the cases of small radial velocity, the poor quality of radar data or the non-standard data preprocessing will result in less satisfactory performance of these methods. Because the wind shear is a form of wind field's unevenness, the error of wind retrieval would be more serious when the variation of wind field becomes large. In this paper, existing wind shear identification and calculation methods are analyzed. Based on the wind retrieval technique and using the uniform wind field model with the VVP (Volume Velocity Process) method, which is employed to examine the unevenness in wind field, the wind shear is identified by calculating the radial velocity gradient between adjacent grids.

2 A BRIEF INTRODUCTION TO VVP TECHNIQUE

2.1 *VVP method and wind field model*

The analysis volume is a 3D space containing several PPI observations in the VVP wind retrieval method [14]. Because the analysis volume is a 3D region, the wind field model of VVP method is suitable to use in high elevations or in the cases of analysis volumes with large width in the vertical direction. Besides, the hypothesis adopted for the analysis volume is that the wind field varies linearly and remains constant during radar scanning.

Considering the radar as the center in the Cartesian coordinate frame, the center coordinate of the analysis volume is (x_0, y_0, z_0), and the velocity of this point is $V=(u_0, v_0, w_0)$. Thus, the velocity onto each point of the analysis volume can be expressed as follows:

$$\begin{cases} u=u_0+u_x(x-x_0)+u_y(y-y_0)+u_z(z-z_0) \\ v=v_0+v_x(x-x_0)+v_y(y-y_0)+v_z(z-z_0) \\ w=w_0+w_x(x-x_0)+w_y(y-y_0)+w_z(z-z_0)+w_f \end{cases} \quad (1)$$

where w_f is the terminal velocity of raindrop

According to the projection between wind field and radar radial direction, the radial velocity measured by radar is:

$$V_r=u\cos\varphi\sin\theta+v\cos\varphi\cos\theta+w\sin\varphi \quad (2)$$

where θ and φ are the azimuth and elevation angles, respectively.

u_0, v_0, w_0, u_x, u_y, u_z, v_x, v_y, v_z, w_x, w_y and w_z are the fit parameters of wind field which are to be retrieved, the corresponding variables in Eq.(2) are defined as:

$$P=[p1, p2, \cdots\cdots p12]=[H_x, H_y, H_z, dxH_x, dyH_x, dzH_x, dxH_y, dyH_y, dzH_y, dxH_z, dyH_z, dzH_z] \quad (3)$$

where $\begin{bmatrix} H_x \\ H_y \\ H_z \end{bmatrix}=\begin{bmatrix} \cos\varphi\sin\theta \\ \cos\varphi\cos\theta \\ \sin\theta \end{bmatrix}$, $\begin{bmatrix} d_x \\ d_y \\ d_z \end{bmatrix}=\begin{bmatrix} x-x_0 \\ y-y_0 \\ z-z_0 \end{bmatrix}$

Thus, one can write:

$$PX=V_r \quad (4)$$

with

$$X=(P^TP)^{-1}P^TV_r \quad (5)$$

For the analysis volume, Eq.(5) can be simplified as:

$$X=A^{-1}B \quad (6)$$

where

$$A=\sum_{i=1}^{N}(P_i^TP_i)=\sum_{i=1}^{N}\begin{bmatrix} p1_i\times p1_i & p2_i\times p1_i & p3_i\times p1_i & \cdots & p11_i\times p1_i & p12_i\times p1_i \\ p1_i\times p2_i & p2_i\times p2_i & p3_i\times p2_i & \cdots & p11_i\times p2_i & p12_i\times p2_i \\ p1_i\times p3_i & p2_i\times p3_i & p3_i\times p3_i & \cdots & p11_i\times p3_i & p12_i\times p3_i \\ \cdots & \cdots & \cdots & \cdots & \cdots & \cdots \\ p1_i\times p11_i & p2_i\times p11_i & p3_i\times p11_i & \cdots & p11_i\times p11_i & p12_i\times p11_i \\ p1_i\times p12_i & p2_i\times p12_i & p3_i\times p12_i & \cdots & p11_i\times p12_i & p12_i\times p12_i \end{bmatrix}$$

$$B=\sum_{i=1}^{N}(P_i*v_{ri})=\sum_{i=1}^{N}\begin{bmatrix} p1_i\times V_{ri} \\ p2_i\times V_{ri} \\ p3_i\times V_{ri} \\ \cdots \\ p11_i\times V_{ri} \\ p12_i\times V_{ri} \end{bmatrix},$$

$$X^T=[u_0, v_0, w_0, u_x, u_y, u_z, v_x, v_y, v_z, w_x, w_y, w_z].$$

Here, A is the coefficient matrix in the VVP method, N is the number of points in the analysis volume and V_{ri} is the radial velocity on every grid. Furthermore, fitted parameters of the wind field can be obtained by solving Eq. (6). Since the ill-conditioned coefficient matrix always causes large errors in retrieval[14-17], the uniform wind field model, which includes only three fitted parameters (u, v, w) with larger magnitude, is adopted to avoid ill-conditioned coefficient matrix and thus to make sure the calculation smoothness in retrieval[18].

Obviously, the relationship between wind field and radial velocity can be written as:

$$V_r=V_h\cos\delta\theta\cos\varphi+w\sin\varphi \quad (7)$$

where V_h is the horizontal wind velocity, $\delta\theta$ is the

included angle between radar azimuth and horizontal wind, φ is the elevation and w is the falling speed of raindrop.

As seen from Eq. (7), the component of wind velocity on the radial is small when the areas are close to the zero velocity line. Thus, the degree of wind velocity variations cannot be represented by the radial velocity exactly. In addition, it is difficult to identify wind shear by using radial velocity difference and threshold values in the presence of observation error

2.2 *The influence of the analysis volume's size on retrieval*

Because of the limitation in computer accuracy, the calculation errors cannot be cleared away in retrieval. Therefore, in order to reduce the influence of calculation errors, using high-precision computation, modifying and improving wind field model would be helpful in retrieval. In addition, the observation errors of radar azimuth, gate size and radial velocity are inevitable. Therefore, one way to reduce these errors is improving the performance of radar observation and retrieval technique. In practice, processes such as smooth filter and interpolation are employed in the preprocessing procedure generally. However, the hypothesis of these preprocessing methods is based on the wind field models rather than the real wind field. Thus, some information of real wind field would be changed in preprocessing. Moreover, some other false information or model errors produced in such smooth filter or interpretation processes are caused by human factors[19].

The random error in the observation is one of the factors, which mainly influence retrieval precision. In order to analyze the influence of the analysis volume's size on errors in retrieval, the random errors in coefficient matrix elements are analyzed as follows:

$$\varepsilon\left(\prod_{\substack{j=1,\\ j\neq i}}^{n} x_i\right) \approx \sum_{i=1}^{n}\left[\left(\prod_{j\neq i}^{n} x_j^*\right)\varepsilon(x_i)\right] \tag{8}$$

Thus, the relative error is:

$$\varepsilon_{\mathrm{r}}^*\left(\prod_{i=1}^{n} x_i\right) \approx \sum_{i=1}^{n} \varepsilon_{\mathrm{r}}^*(x_i) \tag{9}$$

where the symbol * in Eqs. (8) and (9) indicates approximate values. The relative errors of matrix elements in Eq.(6) are

$$\varepsilon_r^*(A_{mn}) \approx \sum_{i=1}^{N}\left[\varepsilon_r^*(H_{mi}) + \varepsilon_r^*(H_{ni})\right] \tag{10}$$

$$\varepsilon_r^*(B_m) \approx \sum_{i=1}^{N}\left[\varepsilon_r^*(H_{mi}) + \varepsilon_r^*(V_{ri})\right] \tag{11}$$

Obviously, for the errors with a normal or uniform distribution, the precision of retrieval results can be improved by increasing the size of analysis volume, namely,

$$\varepsilon_r^*(A_{mn}) \propto 0, \varepsilon_r^*(B_m) \propto 0 \tag{12}$$

$$\delta A \propto 0;\ \delta B \propto 0 \tag{13}$$

Considering that errors can spread and amplify, it is helpful to reduce errors by increasing the analysis volume size at the beginning of retrieval. In addition, the analysis volume is a large sample including several radial and gates. Enlarging the volume size can not only mitigate random errors, but also introduce more information of wind field.

3 A Test With Simulated Data

Because the component of wind field onto radar radial is different with different azimuth, the angle between wind field and radar radial is

$$\delta\theta = \theta_0 - \theta \tag{14}$$

where θ_0 is the direction of horizontal wind field and θ is the radar azimuth.

The gradient of radial velocity can be expressed as

$$S(\theta) = \frac{\partial V_r}{\partial \theta} = V_h \times \sin\delta\theta \times \cos\varphi \tag{15}$$

The $S(\theta)$ is independent of the vertical velocity and the distance of radar and it can be inferred that the position of maximum value appears near the zero velocity line. After normalization in the radial direction, Eq.(15) can be rewritten as

$$\frac{\partial V_r}{r\partial \theta} = S(\theta)/r \tag{16}$$

According to Eq. (16), it can be shown that the wind shear identification methods, which are based on calculating the gradient of radial velocity, can lead to a misjudgment for the same magnitude wind shear on different ring range. Thus, the magnitude of wind shear would be decreased in the distance manually. Besides, in the absence of gradient of radial velocity, it means the wind field is uneven, which is contrary to the traditional wind shear identification conclusion.

In the test, a uniform wind model, which can be retrieved without model bias, contains only three parameters (u_0, v_0, w_0). The wind model sets up 10 layers and the interval of elevations is 1°. The number of radar radials is 360 and the interval is 1°. In each radar radial, there are 460 gates with the each gate length of 250 m. The range of (u_0, v_0, w_0) is (3.0 m/s, 3.0 m/s, 0.5–10.0 m/s), respectively.

As shown in Table 1, the maximum adjacent radial velocity's difference (ARVD) appears at 135° which is perpendicular to the wind field. The results confirmed that the radial velocity's difference reached the maximum near the zero velocity line. Although the ARVD decreases with the increasing of elevation, the variation is not obvious. Through an analysis of the ARVD with changing vertical velocity, it can be inferred that the influence of vertical velocity on wind shear is small for low elevations. In addition, the ARVD changes along with the azimuth, but it remains unchanged at fixed azimuths without normalization processing as mentioned in Eq.(16).

When the wind model of vertical velocity is fixed at (w_0=3.0 m/s), the range of (u_0, v_0) is 3.0–30.0 m/s and

the azimuth of maximum ARVD (as shown in Table 2) is 135°. The value of ARVD, which is consistent with the conclusions of Eq.(15), decreases at high elevations.

Since the resolution of WSR-98D is 0.5 m/s, the random observation error, added on each radial gate in the test, was set to the same as the radar's resolution. In the retrieval, the analysis volume size is 10° × 20 gates and two elevations.

As shown in Table 3, the maximum error of horizontal wind velocity and wind direction is about 3.1 m/s and 10°, respectively. The variation of retrieval error is not obvious in different elevations. It can be inferred that the performance of VVP method is insensitive to elevations.

Table 1. The position (azimuth = 135°) and the maximum adjacent radial velocity difference with fixed horizontal velocity and changing vertical velocity w_0. (u_0=3.0 m/s, v_0=3.0 m/s, R=100 km, elevation: φ).

φ	w_0				
	0.5 m/s	1.0 m/s	3.0 m/s	5.0 m/s	10.0 m/s
1°	0.0740	0.0740	0.0740	0.0740	0.0740
3°	0.0740	0.0740	0.0740	0.0740	0.0740
5°	0.0738	0.0738	0.0738	0.0738	0.0738
7°	0.0735	0.0735	0.0735	0.0735	0.0735
9°	0.0731	0.0731	0.0731	0.0731	0.0731

Table 2. The position (135°) and the maximum adjacent radial velocity's difference with changing horizontal velocity and fixed vertical velocity w_0. (w_0=3.0 m/s, R=100 km, elevation: φ).

φ	u_0, v_0 (u_0=v_0)				
	3.0 m/s	5.0 m/s	10.0 m/s	20.0 m/s	30.0 m/s
1°	0.0740	0.1234	0.2468	0.4936	0.7404
3°	0.0740	0.1233	0.2465	0.4931	0.7396
5°	0.0738	0.1229	0.2459	0.4918	0.7377
7°	0.0735	0.1224	0.2449	0.4898	0.7347
9°	0.0731	0.1218	0.2435	0.4870	0.7305

Table 3. The maximum error of horizontal velocity and the root mean square error of wind direction in retrieval result.

φ	u_0=10.0 m/s, v_0=10.0 m/s, w_0 = 3.0 m/s, σV_r = 0.5 m/s	
	Max (dV_h)	Max ($d\theta$)
1°	3.1	10.1°
3°	3.2	9.8°
5°	3.3	10.2°
7°	3.1	10.1°
9°	3.1	10.7°

As mentioned above, the retrieval error is mainly caused by the model errors and observation errors. For the data near the zero velocity line, they always become unusable due to the observation errors as the radial velocity is small and the data quality is poor. However, the tendency of wind field variation could be easily identified by the VVP retrieval results. Furthermore, relatively strong wind causes relatively small influence of observation errors, leading to accurate retrieval results.

4 A TEST WITH REAL WIND FIELD

4.1 *The wind shear identification algorithm and preprocess*

According to the analysis above, it is inferred that it is a more reasonable way to measure the degree of wind variations and evenness by comparing the difference of retrieved wind for each gate with neighboring grids.

As shown in Fig.1, the wind shear was calculated by comparing the center point with 8 neighboring grids. The maximum gradient value of the velocity difference

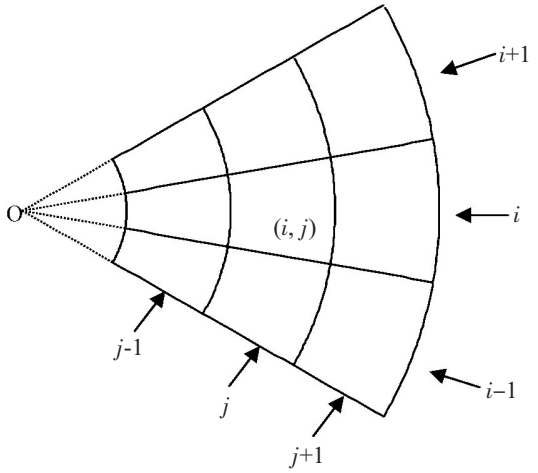

Figure 1. The analysis volume point and its neighboring points.

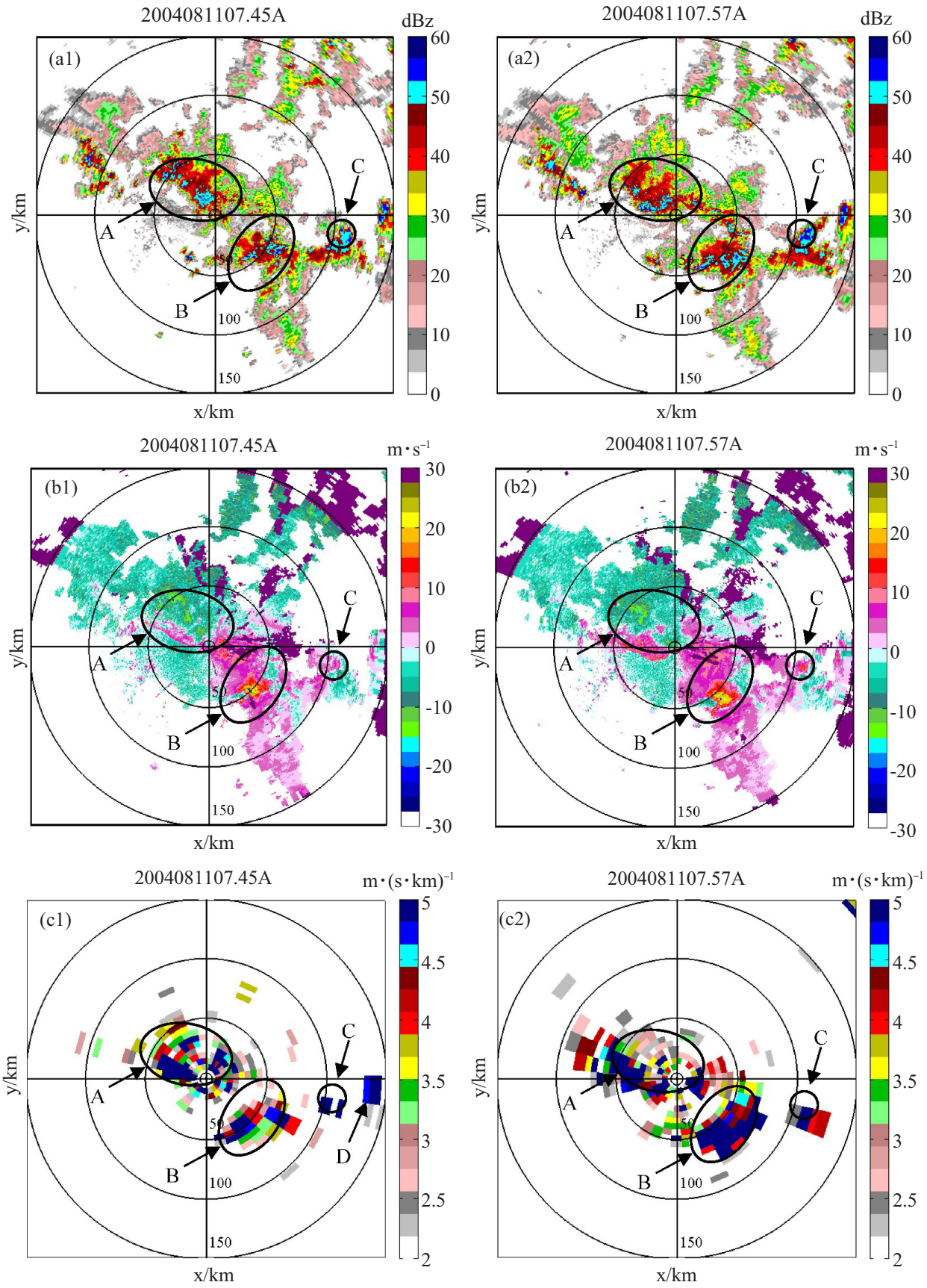

Figure 2. The reflectivity factor (a1–a2), radial velocity (b1–b2) and the wind shear (c1–c2) at 07:45 and 07:57, 11 August, 2004, respectively. Elevation :1.4°.

per unit length was selected to present wind shear magnitude.

In order to ensure the accuracy and completeness of the observation information, the point with the large observation error is rejected instead of smoothing or interpolating in preprocessing. The threshold adopted is

$$S_t = \eta \times (\mathrm{Max}|V_{ri}| - \sum_{i=1}^{N} V_{ri} \Big/ N) \tag{17}$$

Here, η is the weight coefficient with the value of 0.618. N is the number of points in the analysis volume.

4.2 *A test in the process of sever convection weather that happened in Guangzhou*

For the severe convection that happened in Guangzhou, there are three strong echo regions (A, B and C as shown in Fig.2 (a1, a2). The maximum echo exceeds 50 dBZ. Although the formation and moving direction are different in those strong echo regions, it is certain that severe convections existed in these regions and hail might occur.

It can be seen from Fig.2 (b1, b2), all positive and negative radial velocity regions existed in region A and the entire region of strong echoes moved to south-west. In addition, the echoes of low level inflows and gust front are obvious in the moving direction. At the radius range of 50 km in 310°, there was a region with strong wind, it is inferred that convergence and convection developed rapidly there. In region B, strong echoes were moving towards the south. Moreover, the echo area became bigger gradually and then the feature of a meso-cyclone was apparent.

On the contrary, the position of strong echoes seemed steady in region C, but some new strong echoes were generated in the northwest. From the distribution of radial velocity, it can be seen that an anticyclone existed there. Furthermore, the radial velocity increased at the time of b2, implying that the convection developed fast in this region. Based on the identification for wind shear at two times as shown in Fig.2 (c1, c2), i t can be found that the most intensive wind shear appeared in the front of moving direction of strong echoes in region A. The magnitude exceeds 4.5 m/(s·km) and the location is corresponding to inflows in convective cells [20]. In addition, the feature that positive and negative radial velocity coexisted in the same area indicted that the variation of wind field changed intensely.

For region B, the distribution of intensive wind shear was corresponding to that of the meso-cyclone. With the development of the meso-cyclone, the area of wind shear increased at 07:57 than at 07:45 (Fig.2 (b1)). Furthermore, wind shear areas mainly concentrated in the central and front area of the meso-cyclone in the moving path. In the back of the meso-cyclone, the wind field became smooth and the former wind shear regions also disappeared. Because the precipitation particles were limited near the anticyclone in region C, only wind shear located at south side of region C was present and the effective echo area was limited as well. With stronger echoes, the severe wind shear area became larger and moved from the south to the southeast.

According to the variation of echoes, it is found that a new cell was generated in the southeast side of region C. However, since the analysis volume would be enlarged with distance away from radar, the resolution would be decreased. Small convective areas might be included in analysis volume, which lead to the decreased resolution of identification at the same time. For example, as shown in Fig.2(c1), the wind shear area was obvious at 07:45 in region D, but it vanished later at 07:57 with a reduced convection area. The magnitude of wind shear, which existed along with the gust front, divergence or convergence convections and mesocyclones in the severe convection weather in Guangzhou, has exceeded 4.0 m/(s·km) generally. Taking the region B and D in Fig.2 (c1 and c2) as instance, the areas might generate convective cells and the wind shear magnitude exceeded 3.0 m/(s·km).

Consequently, intensive wind shear usually generated in the strong convection, cells and in the front of the moving path of cyclone. Since wind shear areas could increase with severe weather processes, it can be used as a sign to indicate the movements and variation tendency for severe weather processes.

5 CONCLUSIONS

Using radial velocity data of Doppler weather radar, a wind shear identification algorithm was proposed based on the VVP wind retrieval method. According to the error analysis and tests, we draw the following conclusions:

(1) Because the difference in radial velocity varies along with the azimuth in uniform wind field, it reaches the maximum at zero velocity contour. Therefore, wind shear information might be covered or distorted by this phenomenon. The wind shear methods, which are designed based on radial velocity difference, would make misjudgment.

(2) Since wind shear is a presentation of wind field's unevenness, this unevenness is a main factor which would introduce large errors in wind retrieval results. According to the VVP wind retrieval method, a wind shear identification algorithm was proposed by calculating the retrieved wind velocity's difference between neighboring analysis volumes. The larger the wind shear's magnitude is, the more unstable the wind field is.

(3) In the test made with one severe weather process that happened in Guangzhou, for serial cells areas and strong echo areas of mesocyclones, it indicted that wind shear areas mainly distributed in the front of cells and mesocyclones in the moving path. On the contrary, for individual cells, the change of intensive

wind shear area's location was obvious with the generation of new cells. Furthermore, the magnitude of wind shear corresponding to regions of convections and meso-cyclones were larger than others places. It usually exceeded 4.5 m/(s·km) and the moving direction was consistent with those processes accordingly. Besides, if the magnitude of wind shear reaches 3.0 m/(s·km) or above, it implies new convections would be generated. Therefore, the analysis of the location and development of intensive wind shear could be used as a reference in forecasting severe convections.

REFERENCES:

[1] GAO Xiao-rong, LIANG Jian-yin, LI Chun-hui, et al. Radar Quantitative precipitation estimation techniques and effect evalution [J]. J Trop Meterol, 2012, 28(1): 77-88 (in Chinese).

[2] LIU Shu-yuan, YAN Li-feng, SUN Jian. Quality control of single Doppler radar data and retrieval of horizontal wind for a landing typhoon [J]. J Trop Meterol, 2008, 14(2): 115-167.

[3] LI Lei, CHAN Pak-wai, HU Fei et al. Numerical simulation on the wind field structure of a mountainous area beside South China Sea during the landfall of typhoon Molave [J]. J Trop Meteorol, 2014, 20(1): 66-73.

[4] CHEN Qi-zhi, FANG Juan. Effects of vertical wind shear on intensity and structure of tropical cyclone [J]. J Trop Meteorol, 2012, 18(2): 172-186.

[5] RIDDLE A C, HARTTEN L M, CARTER D A, et al. A minimum threshold for wind profiler signal-to-noise ratios [J]. J Atmos Oceanic Technol, 2012, 29(7): 889-895.

[6] SHUN C M, CHAN P W. Applications of an infrared Doppler Lidar in detection of wind shear [J]. J Atmos Oceanic Technol, 2008, 25(5): 637-655.

[7] UYEDA H, ZRNIC D S. Automatic detection of gust fronts [J]. J Atmos Oceanic Technol, 1986, 3(1): 36-50.

[8] HERMES L G, WITT A, SMITH S D, et al. The gust-front detection and wind-shift algorithms for the Terminal Doppler Weather Radar System [J]. J Atmos Oceanic Technol, 1993, 10(5): 693-709.

[9] EILTS M D, OLSON S H, STUMPF G J, et al. An improved gust front detection algorithm for the TDWR[C] // International Conference on Aviation Weather Systems, 4th, Paris, France, Preprints. 1991, 24(28).

[10] MILLER M L, LAKSHMANAN V, SMITH T M. An automated method for depicting mesocyclone paths and intensities [J]. Wea Forecast, 2012, 28(3): 570-585.

[11] AUGROS C, TABARY P, ANQUEZ A, et al. Development of a nationwide, low-level wind shear mosaic in France [J]. Wea Forecast, 2013, 28 (5): 1241-1260.

[12] WANG Nan, LIU Li-ping, XU Bao-xiang et al. Reconizing low-altitude wind shear and convergence line with Doppler radar [J]. J Appl Meterol Sci, 2007, 18(3): 314-320 (in Chinese).

[13] BAI Jian, LI Yong, GAO Xia, et al. Low-level wind shear detection algorithm based on Prony model [J]. Comput Measur Contr, 2009, 10(17): 1889-1890 (in Chinese).

[14] WALDTEUFEL P, CORBIN H. On the analysis of single-Doppler radar data[J]. J Appl Meteorol, 1979, 18(4): 532-542.

[15] BOCCIPPIO D J. A diagnostic analysis of the VVP single-Doppler retrieval technique [J]. J Atmos Ocean Technol, 1995, 12(2): 230-248.

[16] WEI M, DANG R Q, GE W Z, et al. Retrieval single-Doppler radar wind with variational assimilation method-part I: Objective selection of functional weighting factors [J]. Adv Atmos Sci, 1998, 15(4): 553-568.

[17] LI N, WEI M, TANG X, et al. An improved velocity volume processing method [J]. Adv Atmos Sci, 2007 24 (5): 893-906

[18] HOLLENMAN I. Quality control and verification of weather radar wind profiles [J]. J Atmos Ocean Technol, 2005, 22(10): 1541-1550.

[19] ZHOU Sheng-hui, WEI Ming, WANG Li-jun, et al. Sensitivity Analysis of the VVP Wind Retrieval Method for Single-Doppler Weather Radars [J]. J Atmos Ocean Technol, 2014, 31, 1289-1300.

[20] YU Xiao-ding, ZHENG Yuan-yuan, LIAO Yu-fang et al. Observational investigation of a tornadic heavy precipitation supercell storm [J]. Chin J Atmos Sci, 2008, 32(3): 508-522 (in Chinese).

Citation: ZHOU Sheng-hui, WEI Ming, WANG Li-jun et al. Wind shear identification with the retrieved wind of Doppler weather radar [J]. J Trop Meteorol, 2017, 23(2): 210-216.